RESEARCH ARTICLE

INTERNATIONAL RESEARCH JOURNAL OF MULTIDISCIPLINARY TECHNOVATION

Asian Research Association

DOI: 10.54392/irjmt2453

Mechanical and Metallurgical behavior of Manual Metal Arc Welded P91 Ferritic Martensitic Steel Joints

K. Karthick [a, *], K. Vinoth Kumar [a], M. Balasubramanian [b]

[a] Department of Mechanical Engineering, R.M.K. Engineering College, Kavarapetai, Tiruvallur-601206, Tamil Nadu, India.

[b] Department of Mechanical Engineering, R.M.K. College of Engineering and Technology, Puduvoyal, Tiruvallur-601206, Tamil Nadu, India.

* Corresponding Author Email: karthick.kuppan@gmail.com

DOI: https://doi.org/10.54392/irjmt2453

Received: 23-02-2024; Revised: 28-08-2024; Accepted: 07-09-2024; Published: 15-09-2024

Abstract: In the nuclear power plant industry, Cr-Mo ferritic steels are indispensable due to their high-temperature tensile strength, creep strength, and resistance to stress corrosion cracking. This study evaluated and analyzed the mechanical properties and metallurgical behavior of indigenously developed filler (over matched with base metal) manual metal arc welded Cr-Mo ferritic steel (hereafter referred as P91 steel). The analysis revealed that the ultimate tensile properties of the weld joint exceed those of the unwelded metal, being 6% higher than the base metal. Consequently, the joint efficiency for the weld joint is 106%. However, the impact toughness of the weld pad is significantly lower compared to the unwelded metal, nearly 2.5 times less than the base metal. The weld metal region's microstructure is characterized by untempered lath martensite pinned with dense dislocations, which is attributed to rapid cooling from the liquidus range. Furthermore, a distinct Heat-Affected Zone (HAZ) was identified adjacent to the weld metal region, which results from the elevated temperature experienced in this area.

Keywords: P91 steel; Manual Metal Arc Welding; Microstructure; Mechanical Properties

1. Introduction

To increase the effectiveness of the power plants, advanced materials were introduced. Cr-Mo steels like P11, P22, P9, and P91 are widely preferred for the construction of steam headers, pressurizers, and heat exchangers. These steels possess excellent stress corrosion cracking resistance and moderately high-temperature strength. Among various grades of Cr-Mo steels, P91 steel is selected as a potential candidate for ultra-supercritical boilers [1]. This steel is produced in tempered ailment, and it has tempered lath martensitic structure along with fine carbides of V and Nb which retains the strength at high temperature [2]. The joining of materials by welding is unavoidable in power plants. Among the variety of welding processes, Manual Metal Arc Welding (MMAW), Submerged Arc Welding (SAW), Gas Metal Arc Welding (GMAW) and Gas Tungsten Arc Welding (GTAW) processes were preferred due to their reliability and cost effectiveness [3].

The effect of welding consumables on room temperature tensile properties and in-situ microstructure characteristics were studied by Sireesha *et al.* The presence of as welded martensite along with dense dislocations were present in the as fabricated condition. The ductility is reduced to greater extent due to the presence of a small quantity of high temperature ferrite. Tensile properties and microstructural behavior of different soaking temperature (from 973 to 1623 K) were investigated. Tensile properties were correlated with microstructures. Distinct heat affected zone along with varying volume fraction of δ-ferrite were observed for different soaking temperatures. Hardness and tensile properties were found to be decreased in the inter-critical temperature. As strength decreases, the size of prior austenite grain increases. Maximum ductility is obtained for the inter-critical soaking temperature sample [4]. The influence of post weld heat treatment on mechanical properties at room and high temperatures of P91 steel was investigated by Samuel et al. The maximum plastic limit and highest tensile strength decline in a gradual fashion up to midway temperatures followed by a fast change at high temperatures in every heat behavior test [5]. The effect of tempering temperature and austenite stability on toughness were analyzed by Shiue et al. Decrease in impact toughness with a quasi-cleavage fracture pattern was found for the tempering temperature up to 650 °C. After that, a rapid increase in the impact toughness was observed. For weld tempered above 750 °C, the absence of variation in stresses and isothermal change of austenite to martensite were found [6]. Laha et al. investigated the microstructural variation across the weld heat affected zone of P91 steel. A creep test was conducted on the

sample extracted across the weld joint. From this, it was found that an accumulation of creep cavities was found at the interface between HAZ to unwelded metal leading to type-IV cracking [7]. Pandey et al. investigated grain refinement in P92 steel plates using conventional heat treatment (CNT) and double normalized heat treatment (DNT). DNT significantly improved tensile strength without compromising ductility in welded joints compared to CNT Soft δ ferrite formation in weld fusion zones and coarse-grained heat-affected zones was observed, and heat treatment minimized heterogeneity in microstructure and mechanical properties [8]. Kumar et al. prepared a gas tungsten arc welded (GTAW) P91 joint using dissimilar Inconel 617 filler. Optimal strength and ductility were achieved through post-weld normalizing and tempering treatments, with Inconel 617 filler showing higher ductility than P91 filler. Prepared a gas tungsten arc welded (GTAW) P91 joint using dissimilar Inconel 617 filler. Optimal strength and ductility were achieved through post-weld normalizing and tempering treatments, with Inconel 617 filler showing higher ductility than P91 filler [9]. The study conducted by Pandey et al. reviews P91 steel microstructure evolution during heat treatment and creep exposure. Solid solution strengthening, sub-grain hardening, and precipitation hardening contribute to thermal stability. Alloying elements, grain coarsening, Cr/Fe ratio, and dislocation density impact creep rupture life in both base metal and weldments. Lath martensitic microstructure, residual stress, and diffusible hydrogen content also affect P91 steel performance [10]. Sirohi et al. investigated microstructure and mechanical behavior of P22/P91 dissimilar welded joints. Inconel 82 filler exhibited good tensile strength and impact toughness, with safe performance for supercritical power plant applications [11].

From the available literature, it is understood that P91 steel welds were prone to type-IV cracking due to reduced strength zone formation at the interface of the HAZ to unwelded metal [12-21]. However, the mechanism of failure is not completely understood. Hence, the current experimental job is centered on assessing the room-tensile properties and microstructural behavior of P91 steel welds manufactured through the MMAW process with indigenously developed consumble. Additionally, the study aims to discuss the scientific rationale behind the type-IV cracking observed in the joint.

2. Experimental Work

The Modified 9Cr-1Mo (P91) base metal of 25 mm thick is supplied in normalization heat treatment and tempered condition. The chemical composition of P91 base metal was tested in optical emission spectroscopy (OES, Model: Foundry master Xpert) and the details of the test results were discussed in Table 1. The tensile properties like 0.2% offset tensile yield strength, maximum tensile strength, percentage of elongation, reduction of cross-sectional area, and notch tensile strength were evaluated using hydraulic tensile testing machine as per ASTM E8 standard with a strain rate of 1.5 kN/min. Three specimens were tested and the results of the test were furnished in Table 2.

The P91 weld joint was fabricated by MMAW machine (Make: Lincoln Electric, Model: Precision TIG 375). Before welding, the plates were grooved in a double V configuration. In general, the P91 weld joint is vulnerable to hydrogen persuaded cracking, to avoid this the plates were pre-heated to 250 °C before welding and it is checked using thermal crayons. The welding of P91 plates was carried out in a horizontal flat position (1G position) using an E9015-B9 electrode. After welding, the plates were subjected to radiography testing to ensure its soundness. Finally, the welded P91 joint undergoes post weld heat treatment to a specified value and time. The groove details of the joint and weld setup are shown in Figure 1. The constraints used to produce the joints are given in Table 3.

Table 1. Chemical Elements Composition of Cr-Mo Ferritic Steel Base Metal (in wt. %)

C	**Ni**	**Cr**	**Mo**	**Si**	**Mn**	**Cu**
0.105	0.25	9.06	0.79	0.18	0.38	0.041
Nb	**V**	**S**	**P**	**W**	**Al**	**Co**
0.07	0.20	0.017	0.019	0.03	0.01	0.01

Table 2. Tensile Test Results of Base Metal

	0.2% Yield strength (MPa)	UTS (MPa)	Elongation in 50mm gauge length (%)	Reduction in cross sectional area (%)	Notch Tensile strength (MPa)	Notch -Strength –Ratio (NSR)
P91	590±10	720±12	25.3±1.3	69±4	1090±17	1.51

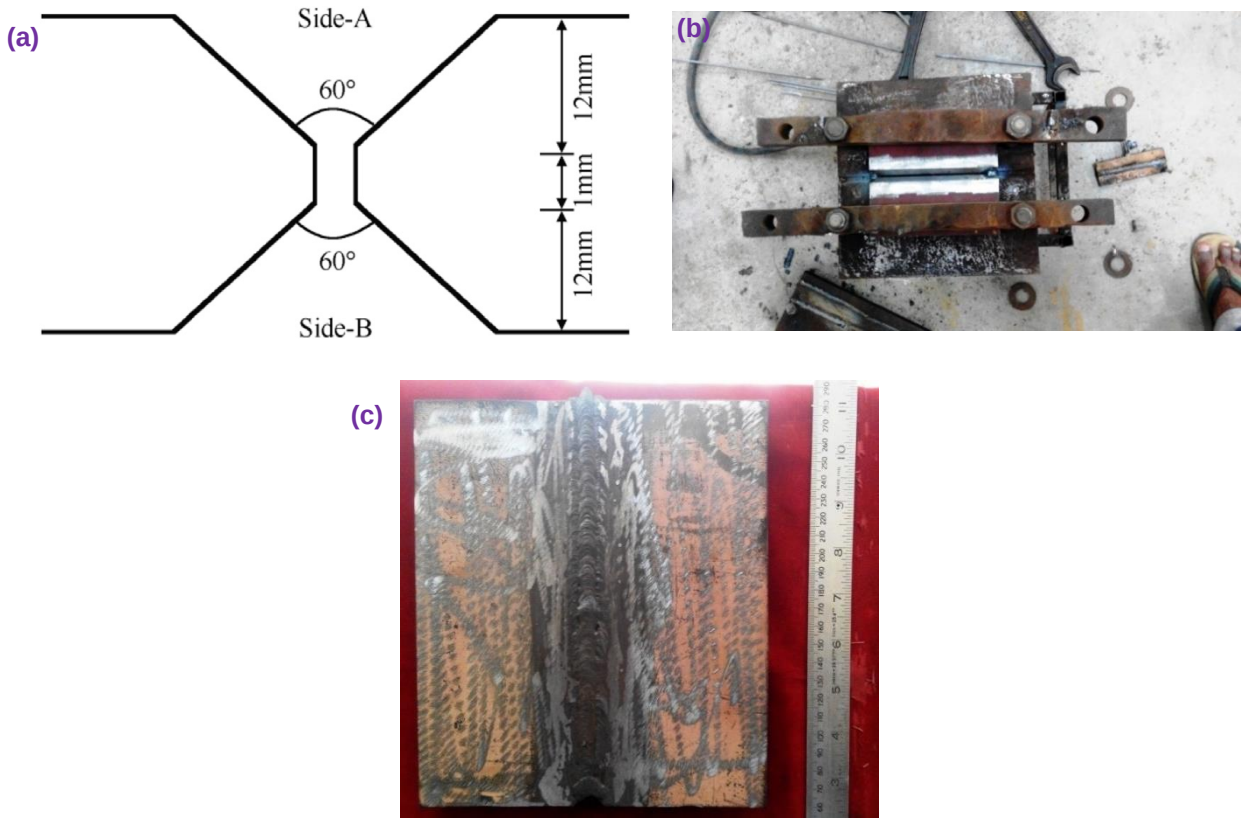

Figure 1 (a) Details of double V configuration, **(b)** Welding Fixture, **(c)** Fabricated P91 Joint

Table 2. Welding Parameters used to Produce the Joint

Process parameters	**P91 Steel**
Current (A)	120
Electrode Designation	E9015-B9
Voltage (V)	22
Filler diameter (mm)	3.15
Travel speed (mm/min)	120
Energy (heat) input (KJ/mm)	1.49
Interpass and preheat	250
SRHT	760 °C for 1h.

The macrostructure of the weld joint was examined using a stereo zoom macroscope. The base metal and weld joint microstructure were examined by optical microscopy (OM) (Make: ZEISS, Model: Met 100T). To reveal the microstructure, the specimens were extracted from base metal and weld joints using a power hacksaw. The extracted specimens were mechanically polished up to 1500 grit size, followed by final polishing using diamond compound (0.25 µm). After polishing, the specimens were etched by Villela's reagent (1 g of picric acid, 5 ml of HCL, and 95 ml of ethanol). The microhardness survey across the weld joint is done by Vicker's microhardness tester (Make: ZEISS, Model: HTV-2T). A 200g load and loading time of 15 seconds were employed for recording hardness values. The tensile properties and charpy impact toughness of the parent metal and weld pad are tested as per the respective standards. For tensile and impact testing, the specimens were extracted normal to the weld joint. For notched tensile test and Charpy impact toughness test, V notch is made in the weld metal. The details of the room temperature tensile and charpy impact toughness specimens were represented in Figure 2. The Photographs of the tensile, notch tensile and impact

toughness specimens (before and after testing) is shown in FIGURE 3. The fractured samples from tensile and impact tests were analysed under scanning electron microscopy (SEM) (Make: JEOL, Model: 4802).

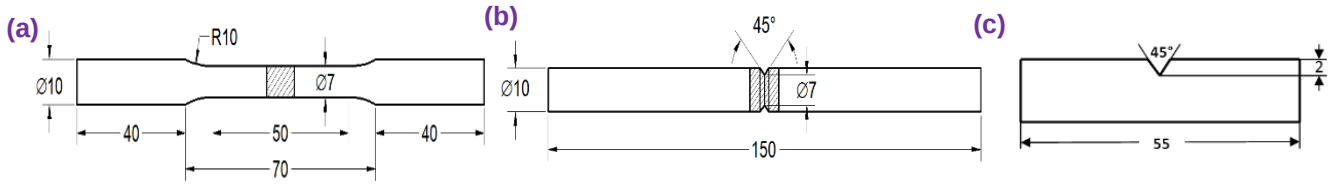

Figure 2. Dimension Details of Cross-tensile and Impact Tougness Specimens

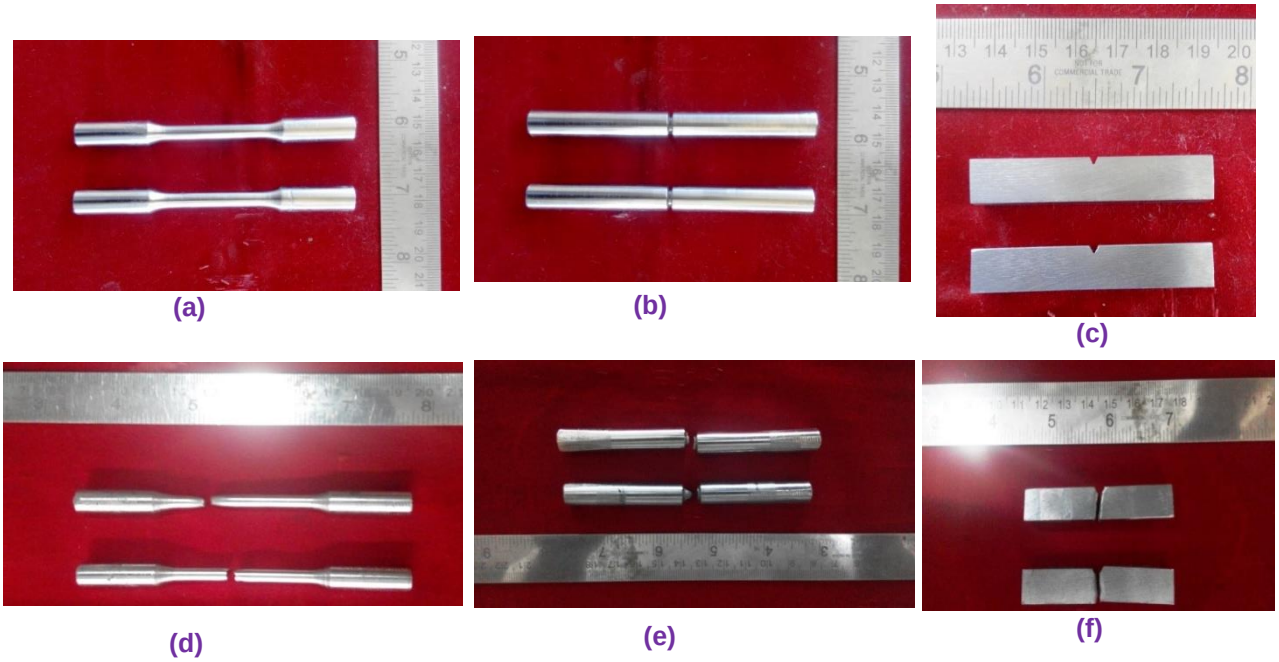

Figure 3. Photographs of tensile, notch-tensile, and impact specimens. (a,b,c) before testing, (d,e,f) after testing

3. Results and Discussion

3.1 Microstructure Analysis

The macrostructure and microstructures of the P91 weld joint were revealed in Figure 4. The macrograph is free from any porosity and other defects and distinct regions like weld metallic region, heat affected zone, and unaffected base metal regions were clearly shown in the Figure 4a. Complete fusion between the base metal and weld metal were evident from Figure 4a. The microstructure of unaffected base metal was revealed in Figure 4b which consists of an over-tempered martensitic structure with prior austenite grain boundary (highlighted using arrow mark in Figure 4b). The as received base metal itself consists of tempered martensite, after welding the joint is exposed to stress relieving weld heat treatment of 760 °C for a duration of 2 hours followed by furnace cooling. During this process the dense dislocations will move freely across the grain boundary and relax the locked in stresses caused during the production process. Fine secondary phase particles that were rich in Cr, Nb, and V are responsible for high temperature strength in this steel. In the P91 steel weld joint, three different heat affected zone were visible, they are intercritical heat affected zone (ICHAZ), fine grain heat affected zone (FGHAZ), and coarse grain heat affected zone (CGHAZ). The local heat recorded in the particular region during welding decides the diverse heat affected zone. The ICHAZ is a region in the heat-affected zone (HAZ) of a weld joint that experiences a peak temperature between the lower critical temperature ($A_{c1}$and the upper critical temperature (A_{c3}). During welding, the ICHAZ undergoes a mixed microstructure transformation. Some of the original austenite grains from the base metal are re-austenitized due to the elevated temperature. These fine re-austenitized grains contribute to the ICHAZ. Additionally, tempered martensite grains retained from the base metal are present in the ICHAZ. The presence of these further-tempered retained grains from the base metal directly influences the hardness reduction observed in the identified soft zone within the as-welded condition. The lower chromium concentrations within these retained grains thermodynamically decrease their potential for austenitic transformation during welding. Heterogeneous grain growth occurs in the ICHAZ during post-weld heat treatment (PWHT) [22]. The region next

to weld metal reaches a temperature well above the upper critical temperature, in this range the secondary phase particles (MX type) liquified in the matrix and allow the grains to grow bigger in size. Hence CGHAZ is formed (Figure 4c).

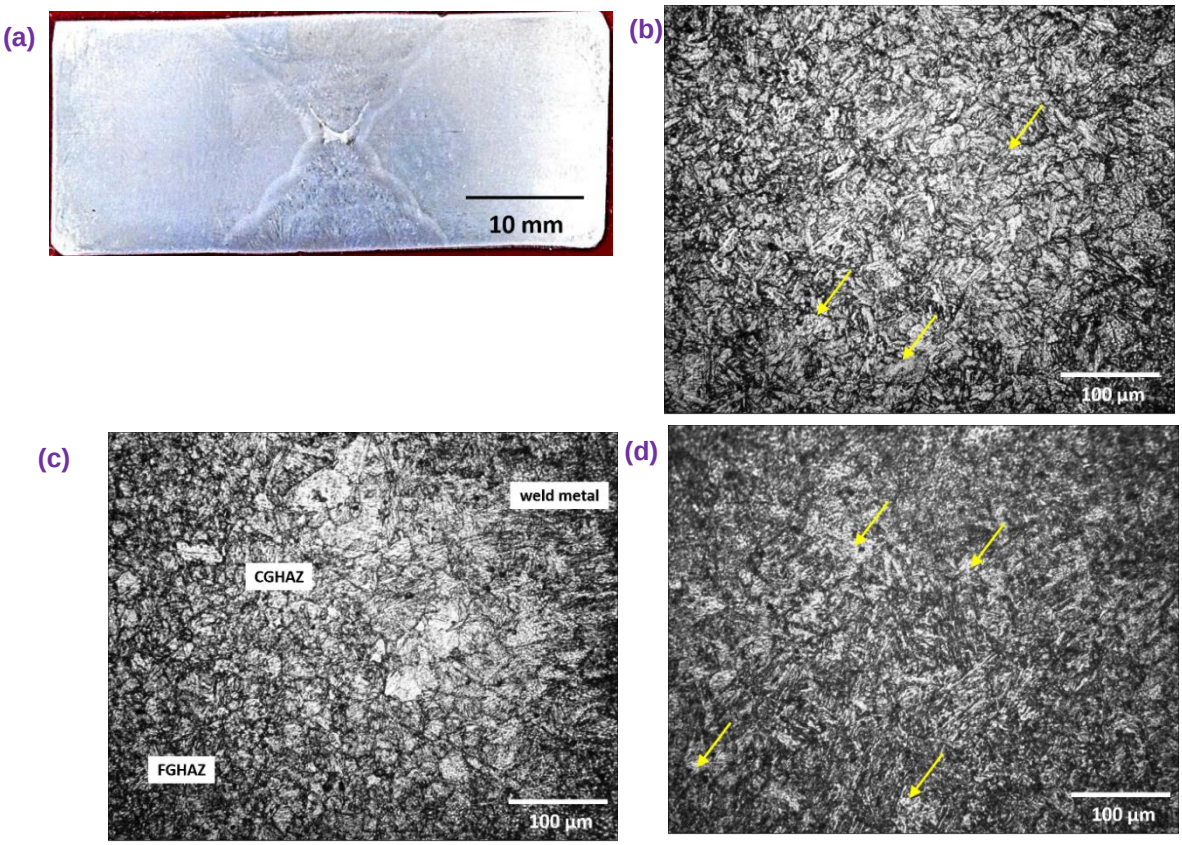

Figure 4. Macrostructure and Microstructures of P91 Weld Joint. (a) Macrograph, (b) P91-Unwelded Metal, (c) Heat Affected Zone, (d) Weld Metal (zone)

The peak temperature experienced adjacent to CGHAZ will not be that much higher, so partial transformation of austenite to martensite occurs, during this process no appreciable grain growth will occur and resulted in FGHAZ (Figure 4c) [10]. In this work, the ICAHZ is not clearly visible. In general, ICHAZ is a very narrow region [usually 50 to 75 µm wide] and mostly appears in single pass welding. The multi-pass welding will cause repeated tempering, so the formation of ICHAZ gets suppressed and can't be visible in this work [23]. The micrograph (optical) of the weld metal region consists of un-tempered lath martensite with small patches of δ-ferrite (highlighted using arrow mark in Figure 2d). The peak temperature in the weld metal region reaches above liquidus temperature, during cooling the liquid transforms to small patches of δ-ferrite along with un-tempered martensite [24].

3.2 Microhardness

Figure 5 shows microhardness dissimilarity crosswise to the welding direction. Peak hardness (~ 400 HV) was observed for weld metal region. The hardness decreases when the distance from the weld metal increases. Again, the hardness is slightly increased when it reached the FGHAZ. The base metal hardness is lowest among all the regions. The microstructure of P91 steel is influenced by heat treatment, which includes normalizing and tempering. The material derives its strength from tempered martensite, dislocation density, and grain boundaries surrounded by $M_{23}C_6$ carbides and MX carbonitrides. During prolonged service, microstructural changes occur, including, Lath widening, Grain coarsening, Precipitate coarsening, and Evolution of intermetallic phases (such as Laves and Z-phase) [11]. The main reason for peak hardness in the welded metal region is due to the existence of an un-tempered martensitic structure along with small patches of δ-ferrite. In the CGHAZ region, the hardness is reduced because of the existence of larger grains compared to FGHAZ [8, 25, 26]. Also, the absence of secondary phase particles in the CGHAZ reduced the value from 400 HV to 346 HV. FGHAZ hardness is slightly higher than CGHAZ because of the partial transformation of retained austenite and martensite along with moderate dislocation density [15, 16]. The hardness remains unchanged in the over-tempered base metal region.

3.3 Cross-Tensile Properties and Charpy's Impact Toughness

Figure 6 depicts the room temperature stress-strain curve for both the Cr-Mo ferritic steel base metal and the

weld joint. Detailed results from the tensile test are presented in Table 4. The data clearly demonstrates that the decisive tensile strength of the weld joint exceeds that of the base metal by 41 MPa. However, the cross tensile specimen extracted from the weld joint fails at the interface between FGHAZ to P91 base metal. Joint efficiency is a parameter used to assess the integrity of the welds represents the ratio of the tensile strength of the welded joint to that of the base metal. In this investigation, a joint efficiency of 106 % was observed. The over-matched weld joint is presented because of the selection of over matching filler metal for better structural integrity of welds [25, 27, 28]. This improved strength was ascribed to the existence of an un-tempered lath martensitic structure (Figure 6d) restrained by a huge number of line defects during welding. The weld metal cools from liquid condition to solid, during this, most of the strengthening particles gets dissolved and re-grows while cooling. The cooling rate of the welding is far higher than regular heat treatment procedures. Hence, the weld zone micrograph seems harder than the unwelded base material. Notch tensile strength was used to estimate the effect of stress concentration on tensile strength and it is used as an indirect parameter in estimating the fracture toughness of the welded joint. The notch tensile strength determined to be greater than that of the base metal. The strength ratio of the notch (NSR) is less than one means the notch is brittle and greater than one means the notch is ductile. From Table 4, it is understood that the notch is ductile since the value is greater than one. Table 5 shows the results of the Charpy V-notch test. It is evident from the data that the impact toughness of the weld joint is significantly inferior to that of the base metal, approximately 2.5 times less than that of the P91 base metal. Even though matched filler metal used in this investigation, small level inclusion and existence of δ-ferrite in the welded metal region will deteriorate the impact toughness to a greater extent. In general, δ-ferrite is a hard phase that has high hardness value but it has poor toughness. The manifestation of small traces of δ-ferrite is evident from Figure 4d along with un-tempered martensite will reduce the impact toughness value.

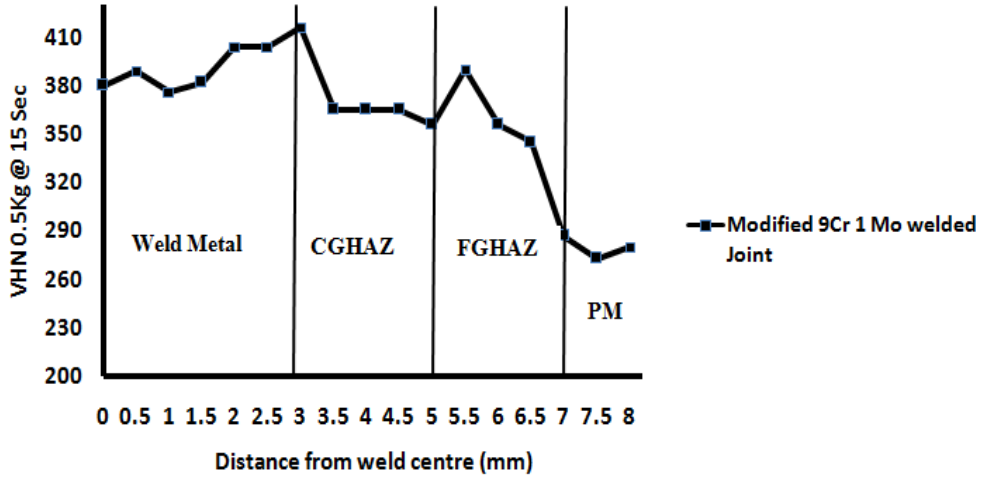

Figure 5. Hardness Variation across the Weld Joint

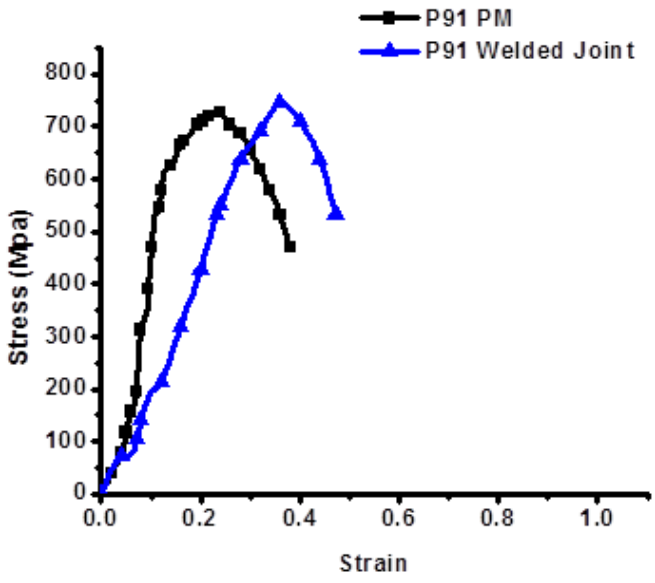

Figure 6. Room Temperature stress-strain curve for BM and weld joint

Table 3. Cross Weld Tensile Results of BM and Weld Joint

	YS (0.2%) (MPa)	UTS (MPa)	Notch Tensile Strength (MPa)	Elongation in 25 mm Gauge length (%)	Notch Strength Ratio (NSR)	Decrease in Cross sectional area (%)	Joint efficiency %	Location of failure
BM	590±10	720±12	1090±17	25.3±1.3	1.51	69±4	---	---
Weld	679±12	761±16	1351±15	12±0.7	1.77	45±2.3	106	HAZ P91 BM interface

Table 4. Impact Toughness of P91 Base Metal and Weld Joint

	Specimen 1	Specimen 2	Specimen 3	Average Impact toughness @ RT (J)
P91 – BM	240	244	240	242
P91 – Weld Joint	76	75	72	74

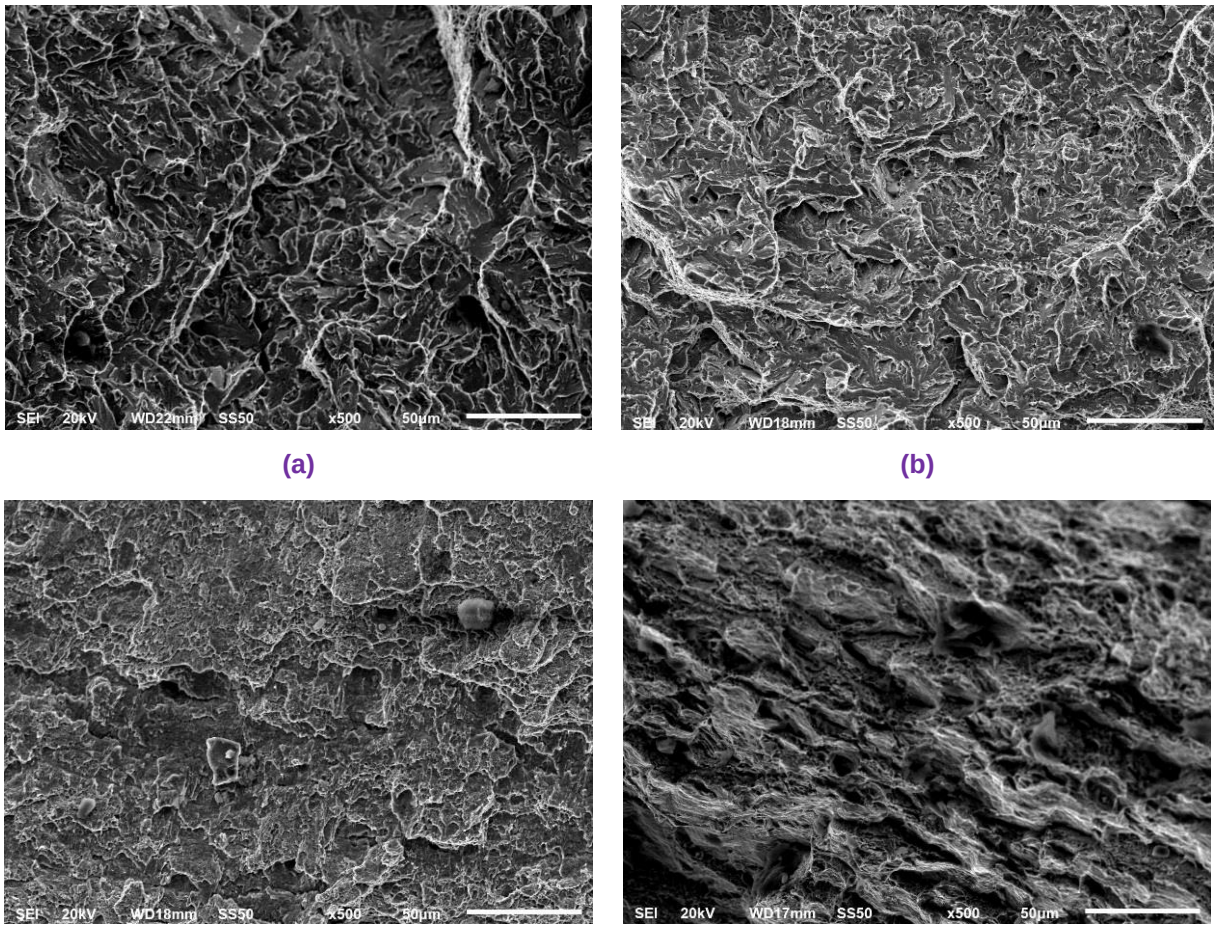

(a) (b)

(c) (d)

Figure 7. Room Temperature stress-strain curve for BM and weld joint

3.4 Fracture Surface Analysis

The fracture surfaces of both room temperature tensile and charpy's impact toughness test samples were shown in Figure 7. The fracture surfaces of cross weld tensile specimens of base metal consist of deeper dimples (Figure 7a) with strong tear ridges whereas the weld joint specimen fracture surface seems very flat and

has small fractions of tear ridges (Figure 7b). From this, it is understood that the ductility and toughness are far better for P91 base metal than for P91 weld joint specimens. The fracture surfaces of impact toughness specimens (Figure 7c and 7d) show stepped fracture and the notch propagates opposite to the loading direction.

Compared to the P91weld joint specimen the base metal specimens have deeper stepped features with large fractions of tear ridges. The stepped feature is irregular for the P91 weld joint specimen and very less fractions of tear ridges were evident. The use of different welding fillers (such as P91 filler) affects the microstructure of the weld fusion zone. Untempered lath martensitic microstructures in the weld fusion zone may lead to poor impact toughness. Understanding the microstructural changes and their impact on fracture surfaces is crucial for ensuring safe weld joints. The fracture surfaces provide critical information about the mechanical properties and behavior of P91 steel weld joints. Ductile fractures are preferred, while brittle fractures can be detrimental. Proper welding practices and heat treatment play a vital role in achieving desirable fracture behavior [5, 11, 29, 30].

4. Conclusions

In this investigation, the mechanical and metallurgical behavior of indigenously developed manually metal arc welded Cr-Mo ferritic steel were examined and discussed. The key findings are as follows:

- The maximum tensile strength exceeds that of the base metal by 6%, resulting in a joint efficiency of 106%. However, it is important to note that the Charpy's impact toughness of the weld joint is considerably lower compared to the base metal. It is nearly 2.5 times less than the base metal.
- The microhardness taken in crossways to the welding direction is heterogeneous in nature. The highest hardness is observed at the weld metal region and the lowest hardness is recorded at the HAZ to base metal interface. This is consistent with the tensile results where the failure location is at the base metal.
- Due to rapid cooling from the liquidus range, the micrograph (optical) of the welded metal region contains un-tempered martensite pinned with dense dislocations. A distinct HAZ was observed adjacent to the welded metal region due to the elevated temperature experienced in this region.
- SEM fracture images of both cross tensile and impact test samples of weld joints seems flat and shallow dimples. The volume fraction of tear ridges is less compared to base metal.

References

[1] A.K. Bhaduri, S. Venkadesan, P. Rodriguez, P.G. Mukunda, Transition metal joints for steam generators-An overview. International Journal of Pressure Vessels and Piping, 58(3), (1994) 251–265. https://doi.org/10.1016/0308-0161(94)90061-2

[2] A.K. Bhaduri, K. Laha, Development of Improved Materials for Structural Components of Sodium-Cooled Fast Reactors. Procedia Engineering, 130, (2015) 598–608. https://doi.org/10.1016/j.proeng.2015.12.276

[3] J.C. Lippold, (2014) Welding Metallurgy and Weldability, Wiley. https://doi.org/10.1002/9781118960332

[4] M. Sireesha, S.K. Albert, V. Shankar, S. Sundaresan, A comparative evaluation of welding consumables for dissimilar welds between 316LN austenitic stainless steel and Alloy 800. Journal of Nuclear Materials, 279(1), (2000) 65–76. https://doi.org/10.1016/S0022-3115(99)00275-5

[5] E.I. Samuel, B.K. Choudhary, K.B.S. Rao, Influence of post-weld heat treatment on tensile properties of modified 9Cr-1Mo ferritic steel base metal. Materials Science and Technology, 23(8), (2007) 992–999. https://doi.org/10.1179/174328407X161295

[6] R.K. Shiue, K.C. Lan, C. Chen, Toughness and austenite stability of modified 9Cr-1Mo welds after tempering. Materials Science and Engineering A, 28(1), (2000) 10–16. https://doi.org/10.1016/S0921-5093(00)00831-5

[7] K.S. Chandravathi, K. Laha, K.B.S. Rao, S.L. Mannan, Microstructure and tensile properties of modified 9Cr-1Mo steel (grade 91). Materials Science and Technology, 17(5), (2001) 559–565. https://doi.org/10.1179/026708301101510212

[8] B. Adhithan, C. Pandey, Study on effect of grain refinement of P92 steel base plate on mechanical and microstructural features of the welded joint. International Journal of Pressure Vessels and Piping, 192 (2021) 104426. https://doi.org/10.1016/j.ijpvp.2021.104426

[9] S. Kumar, C. Pandey, A. Goyal, A microstructural and mechanical behavior study of heterogeneous P91 welded joint. International Journal of Pressure Vessels and Piping, 185, (2020) 104128. https://doi.org/10.1016/j.ijpvp.2020.104128

[10] C. Pandey, M.M. Mahapatra, P. Kumar, N. Saini, Some studies on P91 steel and their weldments. Journal of Alloys and Compounds, 743, (2018) 332–364.

https://doi.org/10.1016/j.jallcom.2018.01.120

[11] S. Sirohi, A. Sauraw, A. Kumar, S. Kumar, T. Rajasekaran, P. Kumar, R.S. Vidyarthy, N. Kumar, C. Pandey, Characterization of Microstructure and Mechanical Properties of Cr-Mo Grade P22/P91 Steel Dissimilar Welds for Supercritical Power Plant Application. Journal of Materials Engineering and Performance, 31, (2022) 7353–7367. https://doi.org/10.1007/s11665-022-06747-y

[12] K. Karthick, S. Malarvizhi, V. Balasubramanian, Evolution of Microstructure at the Interface Region Between Parent Metal (Modified 9Cr–1Mo Steel) and Buttering Layer (Alloy 182) in Dissimilar Joints. Journal of Advanced Microscopy Research, 12(3), (2017) 167–172.

[13] K. Karthick, S. Malarvizhi, V. Balasubramanian, Microstructural characterization of dissimilar weld joint between ferritic steel and stainless steel. Materials Science and Technology, 37(15), (2021) 1–13. https://doi.org/10.1080/02670836.2021.1992949

[14] K. Karthick, S. Malarvizhi, V. Balasubramanian, Mechanical properties and microstructural characteristics of rotary friction welded dissimilar joints of rolled homogeneous armor steel and medium carbon steel. Journal of the Mechanical Behavior of Materials, 30(1), (2021) 171–178. https://doi.org/10.1515/jmbm-2021-0017

[15] K. Karthick, S. Malarvizhi, V. Balasubramanian, A. Gourav Rao, Tensile Properties Variation Across the Dissimilar Metal Weld Joint Between Modified 9Cr–1Mo Ferritic Steel and 316LN Stainless Steel at RT and 550 °C. Metallography, Microstructure, and Analysis, 7, (2018) 209–221. https://doi.org/10.1007/s13632-018-0430-9

[16] K. Karthick, S. Malarvizhi, V. Balasubramanian, S.A. Krishnan, G. Sasikala, S.K. Albert, Microstructural Characteristics and Mechanical Properties of Dissimilar Joints of AISI 316LN Austenitic Stainless Steel and Modified 9cr-1Mo Steel. Indian Welding Journal, 50(4), (2017) 39–46.

[17] K. Karthick, S. Malarvizhi, V. Balasubramanian, S.A. Krishnan, G. Sasikala, S.K. Albert, Tensile properties of shielded metal arc welded dissimilar joints of nuclear grade ferritic steel and austenitic stainless steel. Journal of the Mechanical Behavior of Materials, 25(5-6), (2016) 171–178. https://doi.org/10.1515/jmbm-2017-0005

[18] B. Karthick, L. Shrihari, M. Sakthivel, S. Shriram, V. Silambarasan, Effect of Heat Input on the Microstructure and Mechanical Properties of Gas Tungsten Arc Welded AISI 316 Stainless Steel Joints. International Research Journal on Advanced Science Hub, 2(08), (2020) 23-27.

[19] R. Ashok Kumar, K. Karthick, R. Jayasuriya, J. Aswin Kumar, V. Balaji Karthik, Tribological Behaviour of Aluminum Metal Matrix Composites - A Review. IOP Conference Series: Materials Science and Engineering, 923, (2020) 1–12. https://doi.org/10.1088/1757-899X/923/1/012055

[20] K. Karthick, S. Malarvizhi, V. Balasubramanian, S.A. Krishnan, G. Sasikala, S.K. Albert, Tensile and impact toughness properties of various regions of dissimilar joints of nuclear grade steels. Nuclear Engineering and Technology, 50(1), (2018) 116–125. https://doi.org/10.1016/j.net.2017.10.003

[21] K. Karthick, D. Bharathidhasan, R. Ashok Kumar, F. Mohamed Jaffarsha, M. Sreeraam, K. Surya Prakash, Investigation on Mechanical Properties of Aluminum Metal Matrix Composites - A Review. IOP Conference Series: Materials Science and Engineering, 923, (2020) 012058. https://doi.org/10.1088/1757-899X/923/1/012058

[22] Y. Wang, R. Kannan, L. Li, Correlation between Intercritical Heat-Affected Zone and Type IV Creep Damage Zone in Grade 91 Steel. Metallurgical and Materials Transactions A, 49, (2018) 1264–1275. https://doi.org/10.1007/s11661-018-4490-x

[23] A.K. Bhaduri, K. Laha, V. Ganesan, T. Sakthivel, M. Nandagopal, G.V.P. Reddy, J.G. Kumar, V.D. Vijayanand, S.P. Selvi, G. Srinivasan, C.R. Das, A. Nagesha, S. Ravi, P. Parameswaran, R. Sandhya, S.K. Albert, Advanced materials for structural components of Indian sodium-cooled fast reactors. International Journal of Pressure Vessels and Piping, 139–140 (2016) 123-136. https://doi.org/10.1016/j.ijpvp.2016.02.027

[24] T. Jayakumar, M.D. Mathew, K. Laha, High temperature materials for nuclear fast fission and fusion reactors and advanced fossil power plants. Procedia Engineering, 55, (2013) 259–270. https://doi.org/10.1016/j.proeng.2013.03.252

[25] G. Dak, C. Pandey, A critical review on dissimilar welds joint between martensitic and austenitic steel for power plant application. Journal of Manufacturing Processes, 58, (2020) 377–406. https://doi.org/10.1016/j.jmapro.2020.08.019

[26] C. Pandey, A. Giri, M.M. Mahapatra, Evolution of phases in P91 steel in various heat treatment conditions and their effect on microstructure stability and mechanical properties. Materials Science and Engineering A, 664(10), (2016) 58–74. https://doi.org/10.1016/j.msea.2016.03.132

[27] P. Parameswaran, K. Laha, Role of microstructure on creep rupture behaviour of similar and dissimilar joints of modified 9Cr-1Mo steel. Procedia Engineering, 55, (2013) 438–442. https://doi.org/10.1016/j.proeng.2013.03.277

[28] S. Nagaraju, J. GaneshKumar, P. Vasantharaja, M. Vasudevan, K. Laha, Evaluation of strength property variations across 9Cr-1Mo steel weld joints using automated ball indentation (ABI) technique. Materials Science and Engineering A, 695, (2017) 199–210.

https://doi.org/10.1016/j.msea.2017.04.021

[29] D.W. Rathod, S. Pandey, P.K. Singh, S. Kumar, Microstructure-dependent fracture toughness (J IC) variations in dissimilar pipe welds for pressure vessel system of nuclear plants. Journal of Nuclear Materials, 493, (2017) 412–425. https://doi.org/10.1016/j.jnucmat.2017.06.038

[30] F.C. Liu, T.W. Nelson, S.L. McCracken, Effect of Post-weld Heat Treatment on Microstructure and Mechanical Properties of Dissimilar Metal Weld Used in Power Plants. Metallurgical and Materials Transactions A, 50, (2019) 2826–2834. https://doi.org/10.1007/s11661-019-05223-y

Authors Contribution Statement

KK contributed to conceptualization, methodology, investigation, writing original draft. KVK contributed to investigation. MB contributed to data curation. MB contributed to resources. All authors read and contributed to the manuscript.

Funding

The authors declare that no funds, grants or any other support were received during the preparation of this manuscript.

Competing Interests

The authors declare that there are no conflicts of interest regarding the publication of this manuscript.

Data Availability

The data supporting the findings of this study can be obtained from the corresponding author upon reasonable request.

Has this article screened for similarity?

Yes

About the License